Progress In Electromagnetics Research M, Vol. 91, 123–134, 2020

A Novel Compact Tri Band Notched UWB Monopole Antenna

Venkata N. K. R. Devana[1, *] and Avula M. Rao[2]

Abstract—A novel compact ($20 \times 22\,\mathrm{mm}^2$) triple band eliminated monopole antenna for ultra-wideband (UWB) applications is presented. A novel radiating patch with reduced ground plane is utilized for achieving a $-10\,\mathrm{dB}$ impedance bandwidth of 3.28–13.28 GHz. An upper inverted U-shaped slot is introduced into the radiating patch to notch C-band (3.68–4.19 GHz), and a lower inverted U-structured slot is utilized to eliminate WLAN band (5.18–5.82 GHz) interference. The interference due to down link of X-band (7.27–7.87 GHz) is rejected by via hole connected between patch and rectangular strip printed above the defected ground structure. The proposed antenna has nearly stable radiation patterns, and realized gain over UWB frequency range makes it suitable for recent portable wireless communication applications.

1. INTRODUCTION

In 2002, the Federal Communications Commission (FCC) assigned an unlicensed UWB band from 3.1–10.6 GHz for commercial wireless applications. Recently, various types of Printed Monopole Antennas (PMA) are manufactured for high speed, low profile, short range, and wide bandwidth wireless technologies. Many monopole antennas have been reported to obtain UWB bandwidth; however, systems like 5G [1] (3.3–3.7 GHz), Worldwide Interoperability for Microwave Access, WiMAX [2] (3.3–3.6 GHz), C-band [3] (3.7–4.2 GHz), Wireless Local Area Networks, WLAN [4] (5.15–5.825 GHz), down link of X-band satellite communication systems [5] (7.25–7.75 GHz) may cause electromagnetic interference (EMI) with UWB systems. To suppress EMI, discrete band-stop filters are used with UWB antennas; however, it is complex and costly. In [6], an H-structured slot is etched into a maple-leaf shaped radiator to eliminate 5–6.0 GHz frequency band signals. Three semicircular slots into a radiator are etched to reject 5.15–5.825 and 7.25–7.75 GHz bands. A T-structured parasitic element is introduced to notch 4.9–6.1 GHz signals in [7]. In [8], a complementary split ring resonator notches 5–6 GHz frequencies. Moreover, the UWB radiators are designed with single, double, and multiple notched bands [9–12]. To design an effective UWB radiator with compact size and reduced mutual coupling between band eliminated elements, the proposed antenna is designed.

In this article, a novel UWB radiator is etched with two inverted U-structured slots and a via hole to eliminate C, WLAN, and downlink of X bands, respectively. The simulated and measured results of S_{11}, constant realized gain, surface current distribution and nearly stable radiation patterns of proposed antenna are observed over 3.28–13.28 GHz bandwidth. In the following sections, the design procedure and parametric study of proposed antenna are observed.

2. ANTENNA DESIGN AND DISCUSSION

The proposed radiator with microstrip feed is depicted in Figure 1, and the optimized dimensions are given in Table 1. The proposed antenna is printed on an FR-4 substrate with $\epsilon_r = 4.4$ along with a $50\,\Omega$ with a microstrip line of dimension $W_F \times (L_{F1} + L_{F2})$.

Received 10 February 2020, Accepted 6 April 2020, Scheduled 14 April 2020

* Corresponding author: Venkata Naga Koteswara Rao Devana (dvnkrao@gmail.com).
[1] Department of ECE, JNTUA, Anathapuramu, A.P, India. [2] ECE Department, PBRVITS, Kavali, A.P, India.

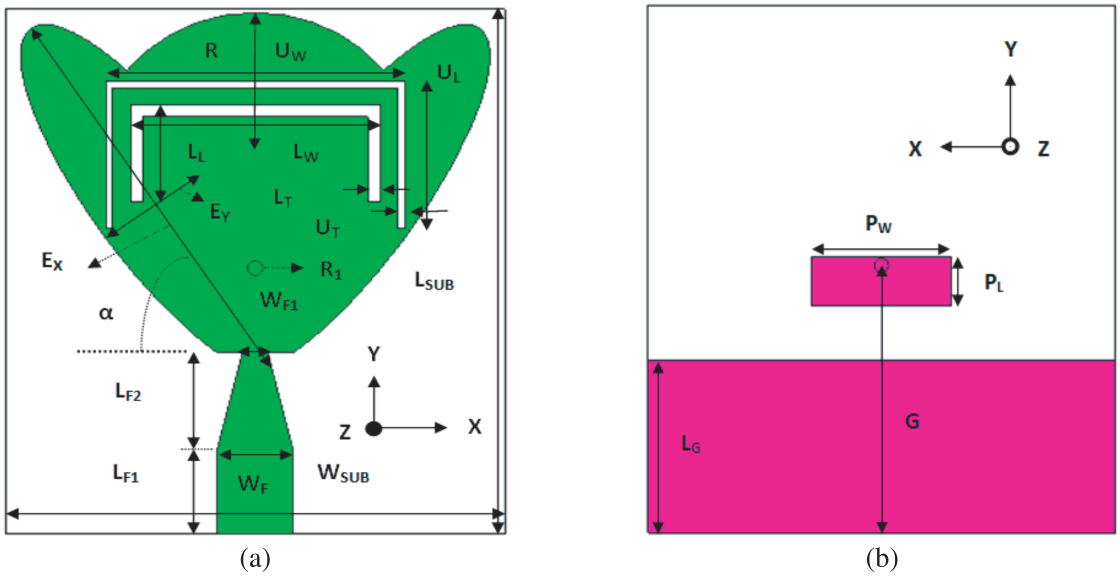

Figure 1. Geometry of the proposed antenna. (a) Top view and (b) bottom view.

Table 1. Dimensions of the proposed antenna.

Parameter	Value (mm)	Parameter	Value (mm)	Parameter	Value (mm)
W_{SUB}	20	R_1	0.3	L_L	4.1
L_{SUB}	22	E_X	2.6	L_T	0.5
W_F	3	E_Y	8.75	L_G	7.2
W_{F1}	1	U_W	12	G	11.15
L_{F1}	3.6	U_L	6.2	P_W	6
L_{F2}	4	U_T	0.3	P_L	2
R	6.5	L_W	10	α	35°

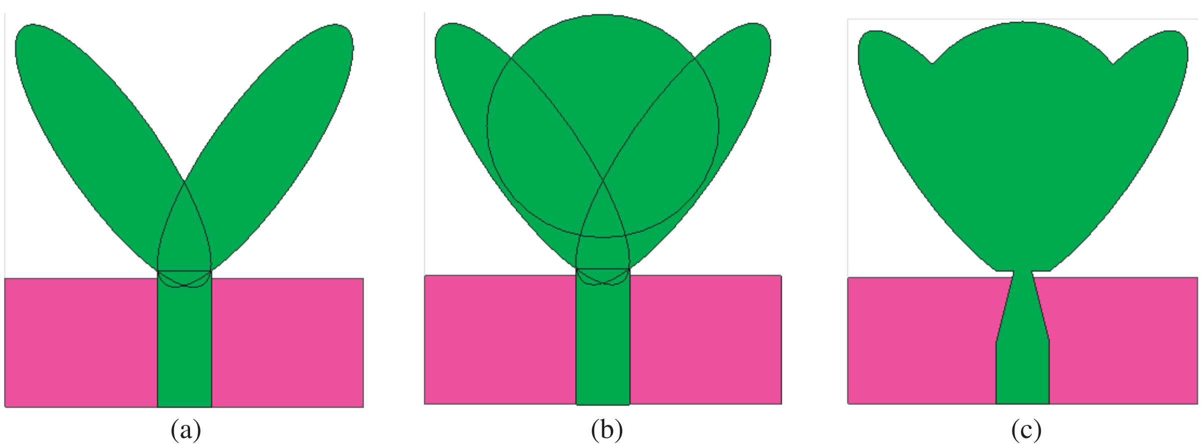

Figure 2. Progressive stages of patch structure. (a) Ant #a. (b) Ant #b. (c) Ant #c.

The progressive stages of basic UWB antenna in achieving UWB bandwidth are depicted in Figures 2(a)–(c). Initially, in the first stage as shown in Figure 2(a), −10 dB impedance bandwidth of 3.71–7.42 GHz is achieved by intersection of two ellipses with major radii of E_X and minor radii of E_Y along with a modified ground structure of $W_{SUB} \times L_G$. In the second stage, the bandwidth is enhanced to 3.56–11.44 GHz by intersecting Ant #a with a circle of radius R to get Ant #b as shown in Figure 2(b). Finally, the microstrip line feed is tapered as shown in Figure 2(c). For structure Ant #c, the bandwidth obtained is from 3.52 to 13.0 GHz as shown in Figure 3.

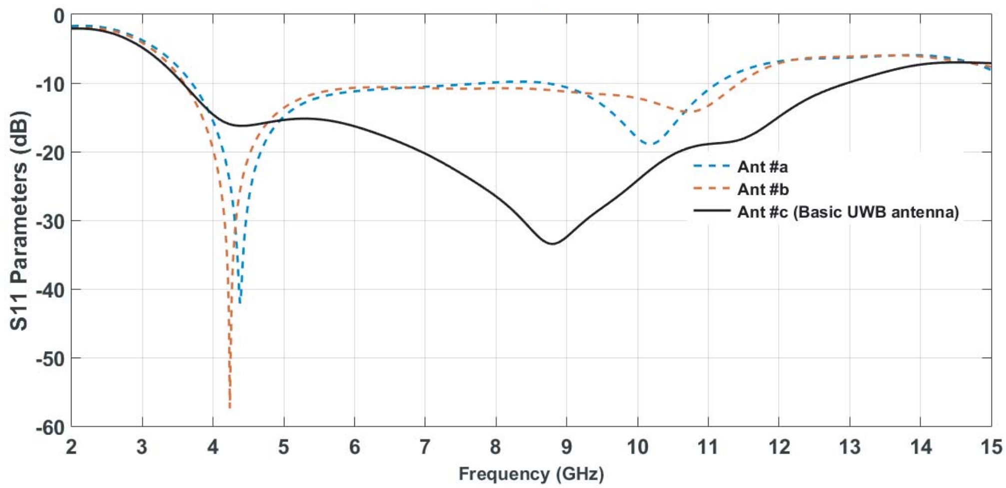

Figure 3. S_{11} plot of basic UWB antenna with varying patch structure.

The variation of angle, α, in steps of 31, 35, and 40 of basic UWB antenna produces impedance bandwidth of 3.52–12.90 GHz, 3.56–12.96 GHz, and 3.63–13.329 GHz with a peak S_{11} of −20.08 dB, −32.44 dB, and −31.32 dB, respectively, as depicted in Figure 4.

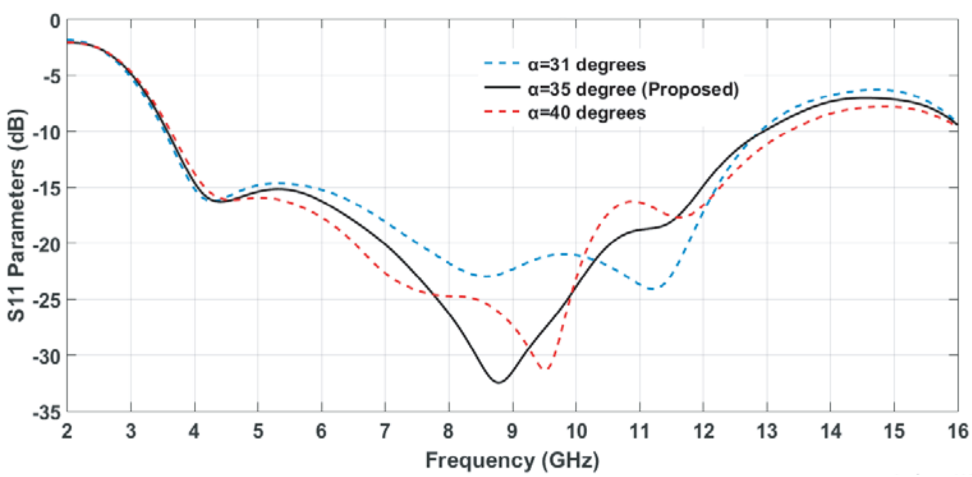

Figure 4. S_{11} plot of basic UWB antenna with varying angle, α.

3. MEASUREMENT RESULTS AND DISCUSSION

The prototype of the proposed antenna is shown in Figure 5. The proposed antenna is simulated by using CST Microwave studio ver.2017, and prototype of antenna is tested by Anritsu MS2037C/2 network analyzer.

The simulated and measured S_{11} plots of the proposed antenna are depicted in Figure 6. From simulation results, it is observed that the band notched antenna has an impedance bandwidth of 3.28–13.28 GHz with triple band notches occurring at 3.68–4.19 GHz for C-band, 5.18–5.82 GHz for WLAN

(a) (b)

Figure 5. Prototype of the proposed antenna. (a) Top view and (b) bottom view.

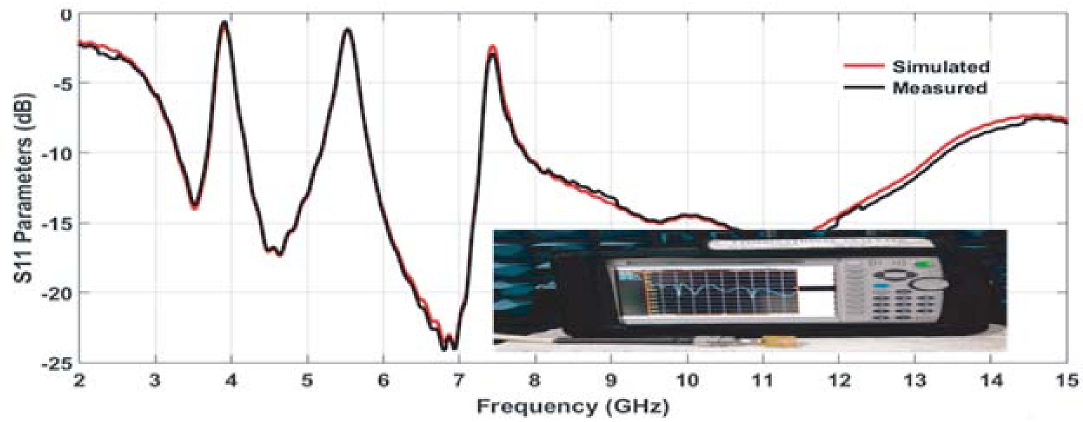

Figure 6. S_{11} plot of proposed UWB band rejected antenna.

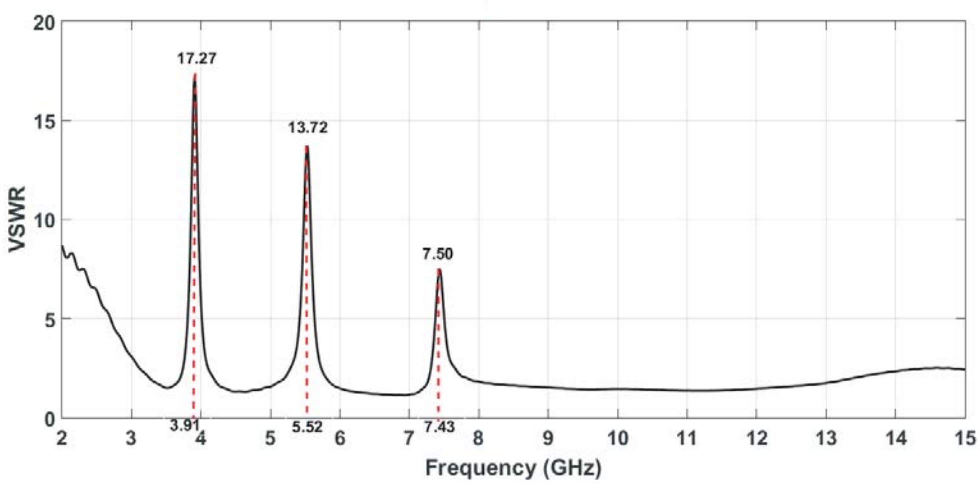

Figure 7. VSWR plot of proposed UWB band rejected antenna.

band, and 7.27–7.87 GHz for down link of X-band applications. A small mismatch between calibrated and simulated results is due to feed misalignments, human measurement errors, and fabrication errors or due to parametric deviations between measured and simulated structures.

The simulated VSWR of proposed antenna is shown in Figure 7. Form Figure 7, it is observed that the proposed antenna has VSWR values of 17.27, 13.72, and 7.50 at three band eliminated frequencies 3.91, 5.52, and 7.43 GHz, respectively. The large VSWR values of proposed antenna indicate that the rejection of notch bands is stronger. The triple band notched characteristics of proposed radiator with parametric study are discussed in the next sections.

3.1. UWB Antenna with C Band Rejection

The C band signals are eliminated by etching an upper inverted U-structured slot into the radiating patch with width U_W, length U_L, and thickness U_T. The slot acts as a half wavelength resonator to notch C band signals and is approximated by using [13],

$$f_{n\_C\,band} = \frac{C}{2\sqrt{\frac{\epsilon_r + 1}{2}}(U_W + 2U_L)} \tag{1}$$

Here C is the speed of light.

When the value of $U_W + 2U_L$ is varied in steps of 23.4 mm, 24.4 mm, and 25 mm with $U_T = 0.3$ mm, and the notched bands occur at 3.87–4.29 GHz, 3.68–4.19 GHz, and 3.55–4.11 GHz ranges of frequencies with centre eliminated frequencies of 4.10, 3.91, and 3.78 GHz, respectively. The reflection coefficient, S_{11}, plots with varying slot length $U_W + 2U_L$ are depicted in Figure 8.

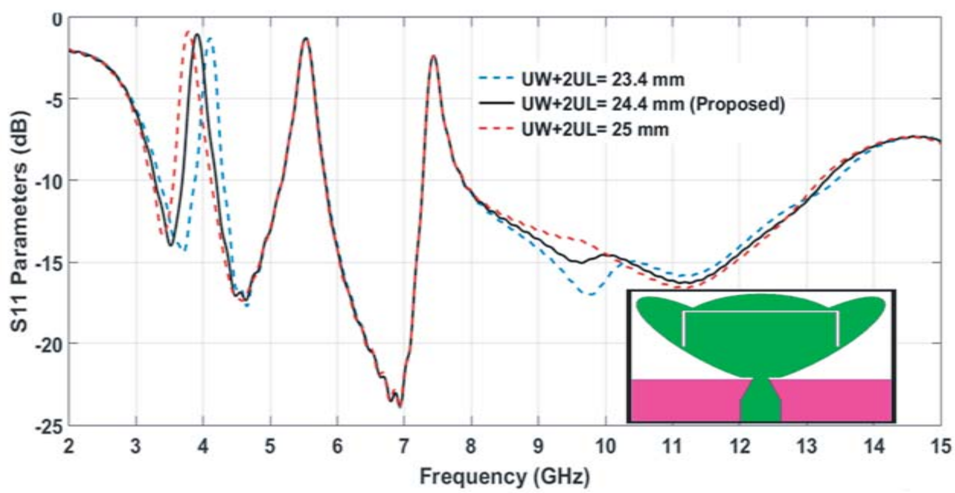

Figure 8. S_{11} plot of proposed antenna with varying upper slot.

3.2. UWB Antenna with WLAN Eliminated Band

To eliminate signals due to WLAN band, the radiating patch is etched with a lower inverted U-structured slot with width L_W, length L_L, and thickness L_T. The lower inverted U-structured slot also acts as a half wavelength resonator to notch 5.49–6.11 GHz, 5.18–5.82 GHz, and 4.89–5.55 GHz bands of frequencies with centre frequencies of 5.83 GHz, 5.52 GHz, and 5.52 GHz when the total length of slot is varied in steps of $L_W + 2L_L = 17.2$ mm, 18.2 mm, and 19.2 mm, respectively. The reflection coefficient, S_{11}, plots with varying slot length $U_W + 2U_L$ are depicted in Figure 9.

The % of magnitude error in slot lengths and eliminated band frequencies are shown in Table 2.

The mutual coupling, S_{21}, between two band notched U-structured slots is depicted in Figure 10. Form Figure 10, the peak value of mutual coupling, S_{21}, between upper and lower inverted U-structured slots is -50.23 dB when $U_W + 2U_L = 24.4$ mm, $L_W + 2U_L = 19.2$ mm, $U_T = 0.3$ mm, $U_L = 0.5$ mm. With $U_W + 2U_L = 25$ mm, $L_W + 2U_L = 18.2$ mm, $U_T = 0.3$ mm, $U_L = 0.5$ mm, the peak value of S_{21} is -63.55 dB; S_{21} is -56 when $U_W + 2U_L = 24.4$ mm, $L_W + 2U_L = 18.2$ mm, $U_T = 0.5$ mm, $U_L = 0.5$ mm; and for the proposed antenna when $U_W + 2U_L = 24.4$ mm, $L_W + 2U_L = 18.2$ mm, $U_T = 0.3$ mm, $U_L = 0.5$ mm, the peak value of mutual coupling is -70.52 dB. The low value of mutual coupling between upper and lower inverted slots indicates that C and WLAN eliminated bands are tuned and

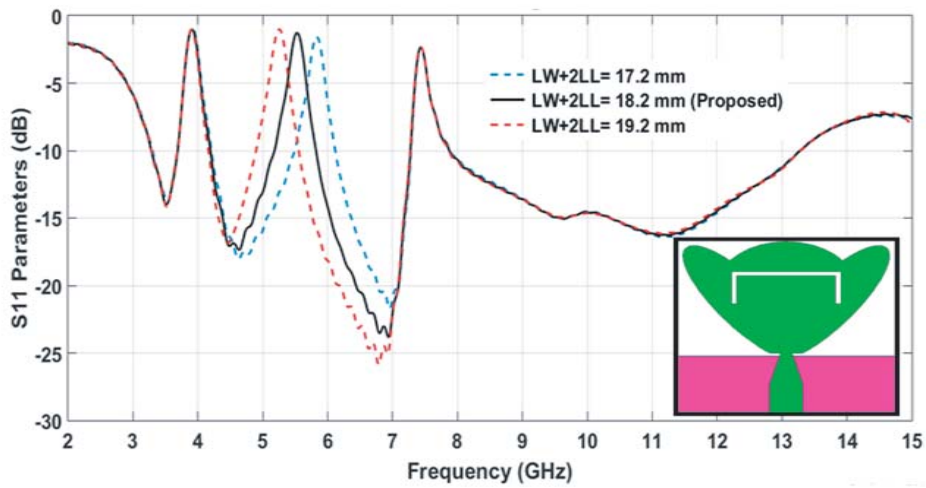

Figure 9. S_{11} plot of proposed antenna with varying lower slot.

Table 2. Magnitude of% error between designed and simulated parameters of slots.

Bandwidth, (GHz)		% bandwidth error	Centre frequency of Notch, (GHz)		Simulated total length of slot, (mm)	Designed total length of slot, (mm)	% error in length of slots
Theoretical	Simulated		Designed	Simulated			
C band (3.7–4.2)	3.69–4.19	0.27, 0.23	3.95	3.91	$U_W + 2U_L = 24.4$	25.31	3.5
WLAN band (5.15–5.825)	5.18–5.82	0.58, 0.08	5.48	5.52	$L_W + 2U_L = 18.2$	18.24	.21

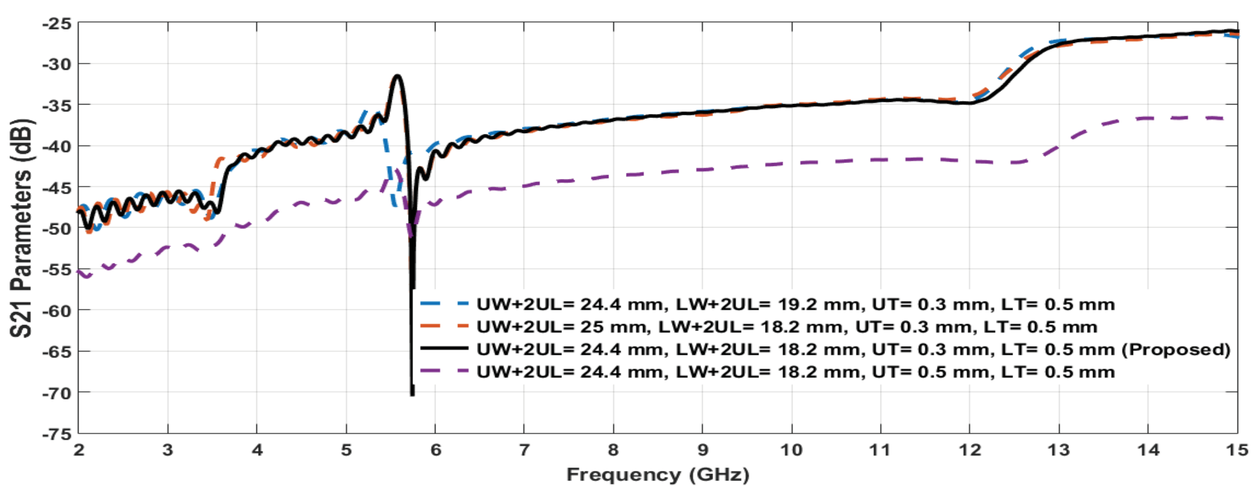

Figure 10. S_{21} plot of proposed antenna with varying slot dimensions.

controlled independently for the proposed radiator [14]. Thus, to suppress interference from C-band and WLAN band more strongly, the thickness of upper inverted U-structure slot is $U_T = 0.3$ mm, and lower inverted U-structured slot is $L_T = 0.5$ mm. In Table 3, the mutual coupling, S_{21}, between two band notched inverted U-structured slots is tabulated.

Table 3. Mutual coupling (S_{21}) between upper and lower U-slots.

Upper U-slot length, $U_W + 2U_L$ (mm)	Lower U-slot length, $L_W + 2U_L$ (mm)	Upper slot thickness, U_T (mm)	Lower slot thickness, L_T (mm)	Peak value of mutual coupling between slots, S_{21} (dB)
24.4	19.2	0.3	0.5	−50.23
25	18.2	0.3	0.5	−63.55
24.4	18.2	0.3	0.5	−70.52 (Proposed)
24.4	18.2	0.5	0.5	−56.0

3.3. Basic UWB Antenna with X Band Eliminated Band

The down link of X-band satellite communications signal is eliminated by using a via hole connected in between a rectangular strip of $P_W \times P_L$ mm^2 deposited on the top surface of defected ground structure and radiating patch. A via hole eliminates 7.27–7.87 GHz of frequency band by preventing the current from radiating patch on top of the substrate to the rectangular parasitic strip under the substrate [15]. The X-band is tuned by varying radius, $R_1 = 0.25$ mm, 0.3 mm and 0.35 mm to achieve the rejected bands from 7.02–7.48 GHz, 7.27–7.87 GH,z and 7.52–8.27 GHz with centre of notch frequencies at 7.16 GHz, 7.43 GHz, and 7.72 GHz, respectively, as depicted in Figure 11.

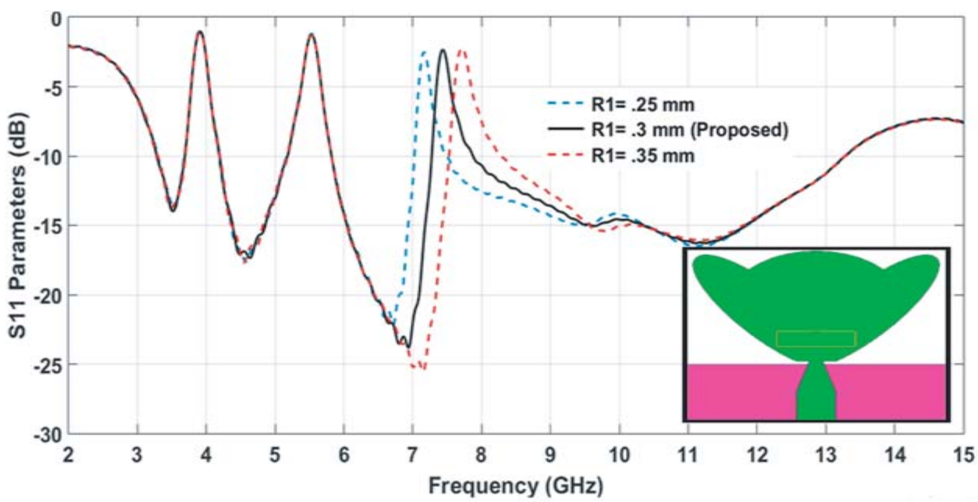

Figure 11. S_{11} plot of proposed antenna with varying via radius, R.

When the value of gap G, between bottom of substrate and the centre of via, is varied in steps of 9.85 mm, 10.15 mm, and 11.15 mm, the centre of eliminated bands occurs at 7.36, 7.57, and 7.43 GHz with rejected frequency bands from 7.14–7.92, 7.35–8.19, and 7.27–7.87 GHz as depicted in Figure 12.

The parametric study of proposed antenna with variation of parameters of slots and via is depicted in Table 4. In Table 4, it is observed that the variation of parameters of band notched elements of proposed radiator, notch frequency, resonant frequency, VSWR, and simulated bandwidth, are tuned. The proposed antenna is optimized to achieve minimum value of % error in calibration of theoretical and simulated bandwidths are depicted in Table 4.

3.4. Radiation Patterns, Current Distribution, Realized Gain

The radiation patterns in E-plane and H-plane of proposed antenna are depicted in Figure 13, at resonant frequencies of 3.5, 4.63, and 6.94 GHz. In E-plane, the patterns are nearly like dipole and

Table 4. Parametric study of proposed antenna.

Parameter	value (mm)	Notch frequency, (GHz)	Resonant frequency of notch (GHz)	VSWR at f_n	Theoretical Bandwidth, (GHz)	Simulated Bandwidth, (GHz)	% error in Bandwidth
Upper Slot length, $U_W + 2U_L$	23.4	4.10	3.70	13.71	3.7–4.2 (C band)	3.87–4.29	4.5, 2.1
	24.4 (proposed)	3.91	3.50	17.27		3.68–4.19	0.54, 0.23
	25	3.78	3.40	20.28		3.55–4.11	4.05, 2.14
Lower Slot length, $L_W + 2U_L$	17.2	5.83	4.63	11.12	5.15–5.825 (WLAN)	5.49–6.11	6.6, 4.89
	18.2 (proposed)	5.52	4.62	13.72		5.18–5.82	0.58, 0.08
	19.2	5.25	4.45	17.37		4.89–5.55	5.04, 4.72
Gap, G	9.85	7.36	6.46	7.16	7.25–7.75 (X-band)	7.14–7.92	1.51, 2.1
	10.15	7.57	6.86	7.36		7.35–8.19	1.37, 5.67
	11.15 (proposed)	7.43	6.94	7.50		7.27–7.87	0.27, 1.5
Via radius, R	0.25	7.16	6.71	6.99		7.02–7.48	3.17, 3.48
	.3 (proposed)	7.43	6.94	7.50		7.27–7.87	0.27, 1.54
	0.35	7.72	7.14	7.84		7.52–8.27	3.72, 6.7

omnidirectional in H-plane. The increased magnitude of higher order modes and unequal phase variations of antenna aperture cause more distortion of radiation patterns at higher frequency 6.94 GHz.

The operation of band notch characteristics of proposed radiator can be better understood by the surface current distributions at notch frequencies of 3.92, 5.52, and 7.43 GHz as depicted in Figures 14(a)–(c). More surface currents are concentrated around upper inverted U-structured slot to eliminate C-band at 3.92 GHz frequency, lower inverted slot for rejection of WLAN band at 5.52 GHz, and via for notching down link of X-band satellite communication at 7.43 GHz.

The realized peak gain against frequency for proposed radiator is shown in Figure 15. The gain varies from 2.11 to 5.12 dBi within 3.28–13.28 GHz of frequency band, except for eliminated bands

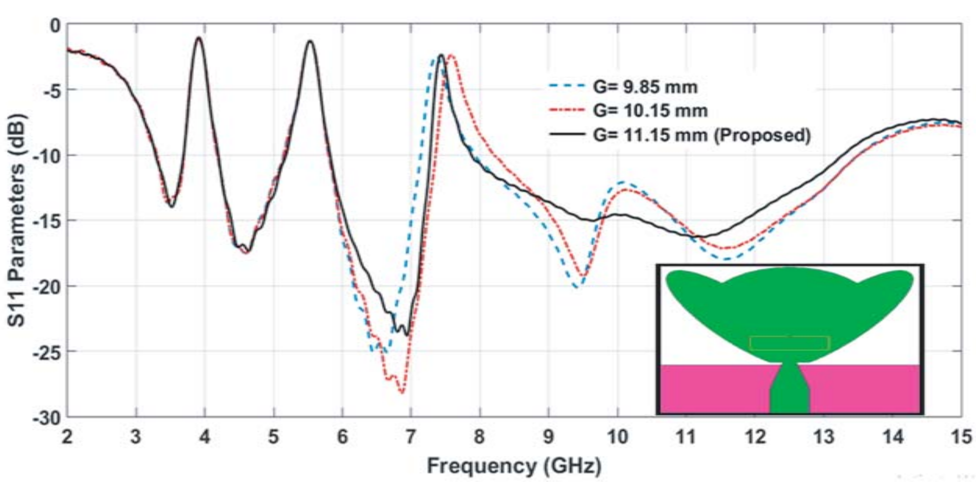

Figure 12. S_{11} plot of proposed antenna with varying gap, G.

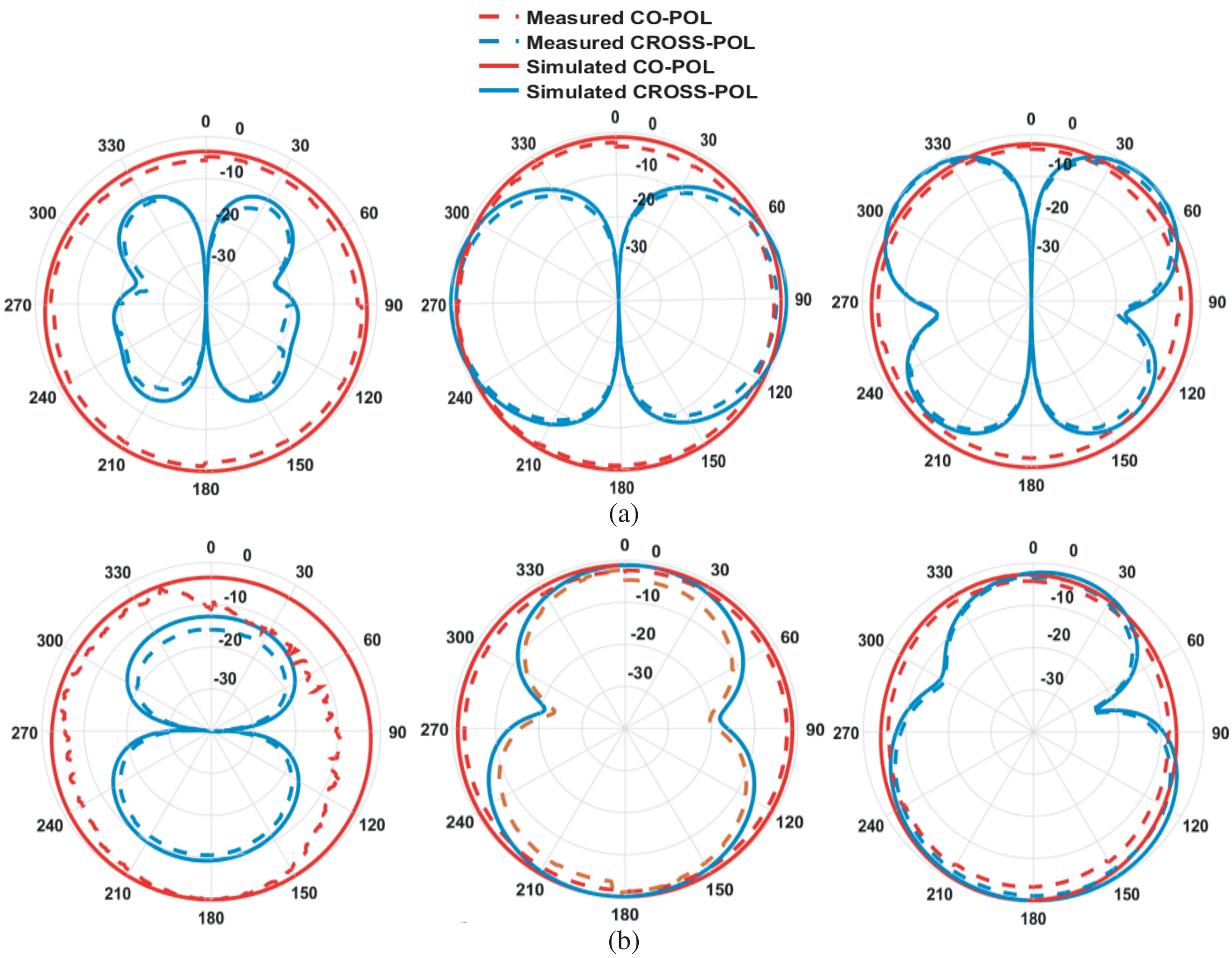

Figure 13. Simulated and measured radiation patterns. (a) E plane at 3.5, 4.63 and 6.94 GHz. (b) H plane at 3.5, 4.63 and 6.94 GHz.

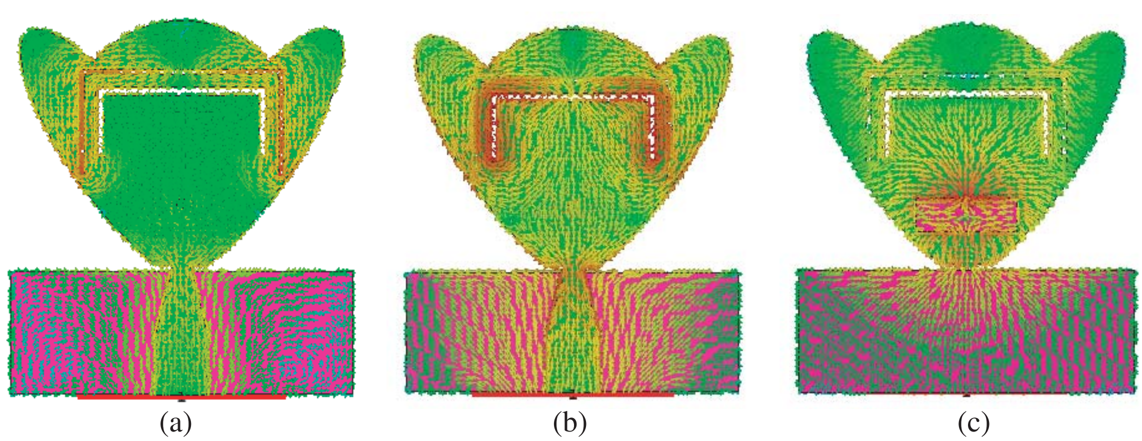

Figure 14. Surface current distributions at notched frequencies (a) 3.92 GHz, (b) 5.52 GHz, (c) 7.43 GHz.

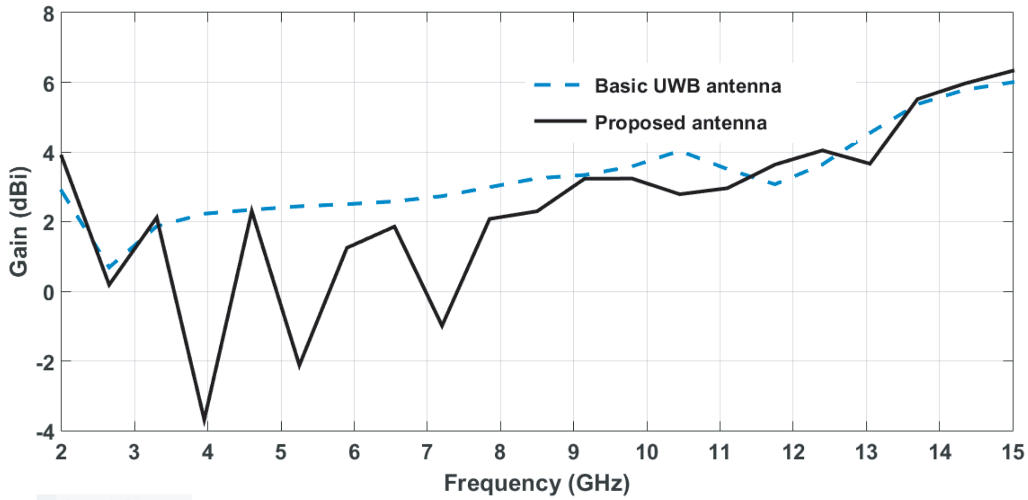

Figure 15. Realized gain of the proposed antenna.

of 3.68–4.19 GHz, 5.18–5.82 GHz, and 7.27–7.87 GHz with centre eliminated frequencies of 3.92, 5.52, and 7.43 GHz to notch C, WLAN, and X-band applications, respectively. The realized peak gains of proposed antenna at notch frequencies of 3.92, 5.52, and 7.43 GHz are −3.82 dBi, −2.16 dBi, and −1.04 dBi, respectively.

The comparison of proposed band notched UWB antenna with other recently reported antennas [16–21] is given in Table 5.

Table 5. Size, bandwidth and VSWR parameter comparison of proposed antenna with recently reported antennas in literature.

Ref. Antennas	Size (mm^2)	Area (mm^2)	Notch Bands (GHz)	Operating frequency, (GHz)	VSWR at notch frequency
[16]	20×26	520	5.15–5.68, 7.15–7.65	3.05–20	6.6, 6.1
[17]	42×50	2100	3–4, 5–6	3.1–10.6	14, 9.5
[18]	42×50	2100	3.3–3.8, 5.15–5.825, 7.1–7.9	2–11	4.8, 5.2, 6.9
[19]	42×50	2100	3.3–3.6, 5–6	2.1–10.8	6, 6.5
[20]	36×34	1224	3.97–4.48, 5.79–6.57, 7.6–7.6	3.1–10.6	11.2, 5.8, 5.6
[21]	27.5×16.5	453.75	2.2–3.9, 5.1–6	1.75–10.3	10, 7.2
This work	20×22	440	3.68–4.19, 5.18–5.82, 7.27–7.87	3.28–13.28	17.27, 13.72, 7.50

4. CONCLUSION

A novel compact monopole antenna for UWB applications with tri band notched characteristics is proposed. The proposed antenna covers fractional bandwidth of 120% (3.28–13.28 GHz) with three band eliminated frequencies from 3.68–4.19 GHz, 5.18–5.82 GHz, and 7.27–7.87 GHz to notch C, WLAN, and down link of X-band applications by etching upper, lower inverted slots into the radiating patch and a via hole, respectively. The proposed antenna has compact size of $20 \times 22\,mm^2$, independently controlled tri band notched characteristics, and stable realized peak gain, and radiation patterns over UWB frequency range make it suitable for portable UWB communication systems.

REFERENCES

1. Elhabchi, M., M. N. Srifi, and R. Touahni, "CPW-fed miniaturized isosceles triangular slot UWB planar antenna with triple band-notched characteristics," *Progress In Electromagnetics Research Letters*, Vol. 87, 59–66, 2019.
2. Tang, M.-C., S. Xiao, T. Deng, D. Wang, J. Guan, B. Wang, and G.-D. Ge, "Compact UWB antenna with multiple band-notches for WiMAX and WLAN," *IEEE Transactions on Antennas and Propagation*, Vol. 59, No. 4, 1372–1376, April 2011.
3. Lotfi, P., M. Azarmanesh, and S. Soltani, "Rotatable dual band-notched UWB/triple-band WLAN reconfigurable antenna," *IEEE Antennas and Wireless Propagation Letters*, Vol. 12, 104–107, 2013.
4. Anagnostou, D. E., M. T. Chryssomallis, B. D. Braaten, J. L. Ebel, and N. Sepúlveda, "Reconfigurable UWB antenna with RF-MEMS for on-demand WLAN rejection," *IEEE Transactions on Antennas and Propagation*, Vol. 62, No. 2, 602–608, February 2014.
5. Alnahwi, F. M. and N. E. Islam, "A generalized concept for band notch generation in ultra-wide band antennas," *Progress In Electromagnetics Research C*, Vol. 54, 179–185, 2014.
6. Ahmed, O. M. H. and A. R. Sebak, "A novel maple-leaf shaped UWB antenna with a 5.0–6.0 GHz band-notch characteristic," *Progress In Electromagnetics Research C*, Vol. 11, 39–49, 2009.
7. Liu, W. X. and Y. Z. Yin, "Dual band-notched antenna with the parasitic strip for UWB," *Progress In Electromagnetics Research Letters*, Vol. 25, 21–30, 2011.
8. Mishra, G. and S. Sahu, "Compact circular patch UWB antenna with WLAN band notch characteristics," *Microwave and Optical Technology Letters*, Vol. 58, No. 5, 1068–1073, May 2016.
9. Jiang, W. and W. Che, "A novel UWB antenna with dual notched bands for WiMAX and WLAN applications," *IEEE Antennas and Wireless Propagation Letters*, Vol. 11, 293–296, 2012.
10. Sarkar, D., K. V. Srivastava, and K. Saurav, "A compact microstrip-fed triple band-notched UWB monopole antenna," *IEEE Antennas and Wireless Propagation Letters*, Vol. 13, 396–399, 2014.
11. Wu, Z.-H., F. Wei, X.-W. Shi, and W.-T. Li, "A compact quad band-notched UWB monopole antenna loaded one lateral L-shaped slot," *Progress In Electromagnetics Research*, Vol. 139, 303–315, 2013.
12. Xu, J., D. Shen, X. Zhang, and K. Wu, "A compact disc ultrawideband (UWB) antenna with quintuple band rejections," *IEEE Antennas and Wireless Propagation Letters*, Vol. 11, 1517–1520, 2012.
13. Mewara, H. S., J. K. Deegwal, and M. M. Sharma, "A slot resonators based quintuple bandnotched Y-shaped planar monopole ultra-wideband antenna," *International Journal of Electronics and Communications*, Vol. 83, 470—478, 2018.
14. Mewara, H. S., D. Jhanwar, M. M. Sharma, and J. K. Deegwal, "A novel hammer-shaped UWB antenna with triple notched-band for rejecting RLS, WLAN and XSCS bands," *Advanced Electromagnetics*, Vol. 6, No. 4, 36–41, October 2017.
15. Zehforoosh, Y., M. Mohammadifar, A. H. Mohammadifar, and S. R. Ebadzadeh, "Designing four notched bands microstrip antenna for UWB applications, assessed by analytic hierarchy process method," *Journal of Microwaves, Optoelectronics and Electromagnetic Applications*, Vol. 16, No. 3, 765–776, September 2017.
16. Mouhouche, F., A. Azrar, M. Dehmas, and K. Djafri, "Compact superformula based ultra-wideband antenna shape with two notched bands," *Microwave and Optical Technology Letters*, 1–5, May 2015.
17. Xi, L., H. Zhai, Y. Zang, and L. Li, "A novel dual-band tunable band-notched antenna," *Microwave and Optical Technology Letters*, Vol. 59, 3014–3018, 2017.
18. Jaglan, N., B. K. Kanaujia, S. D. Gupta, and S. Srivastava, "Triple band notched UWB antenna design using electromagnetic band gap structures," *Progress In Electromagnetics Research C*, Vol. 66, 139–147, 2016.
19. Jaglan, N., B. K. Kanaujia, S. D. Gupta, and S. Srivastava, "Design of band notched antenna with DG-CEBG," *International Journal of Electronics*, Vol. 105, No. 1, 58–72, 2017.

20. Rahman, S. U., Q. Cao, Y. Li, I. Gil, and W. Yi, "Design of tri-notched UWB antenna based on elliptical and circular ring resonators," *International Journal of RF and Microwave Computer-Aided Engineering*, e21648, 2018.
21. Kundu, S., "Balloon-shaped CPW fed printed UWB antenna with dual frequency notch to eliminate WiMAX and WLAN interferences," *Microwave and Optical Technology Letters*, Vol. 60, 1744–1750, 2018.